ChemPlusChem

Research Article
doi.org/10.1002/cplu.202300167

Chemistry Europe
European Chemical Societies Publishing

www.chempluschem.org

Special Collection

Anti-Tumoural [NHC(thiolato)] Gold(I) Complexes Derived from HIF-1α Inhibitor AC1-004 Target the Mitochondrial Redox System and Show Antiangiogenic Effects in vivo

Sebastian W. Schleser[+],[a] Leonhard H. F. Köhler[+],[a] Florian Riethmüller,[a] Sebastian Reich,[a] Robin Fertig,[b] Luca Schlotte,[a] Jonathan Seib,[a] Alexander Goller,[b] Gerrit Begemann,[c] Rhett Kempe,[b] and Rainer Schobert*[a]

AC1-004 is a potent inhibitor of the hypoxia-inducible factor alpha (HIF-1α) pathway, essential for tumour growth, angiogenesis and metastasis. We modelled a series of gold(I) complexes on AC1-004, retaining its 5-carboalkoxybenzimidazole as an NHC ligand while replacing its 2-aryloxymethyl residue with modified thiolato gold(I) fragments. The intention was to augment a potential HIF-1α inhibition by conducive effects typical of NHC gold complexes, such as an inhibition of tumoural thioredoxin reductase (TrxR), an increase in reactive oxygen species (ROS), and cytotoxic and antiangiogenic effects. We report on the synthesis and biological effects of twelve such N,N′-dialkylbenzimidazol-2-ylidene gold(I) complexes, obtained in average yields of 65% for the thiophenolato and 45% for the novel 4-(adamant-2-yl)benzenethiol complexes. The structure of one complex was validated via single-crystal X-ray diffraction. Structure-activity relationships (SAR) were derived by variation of the N-substituents (Me, Et, *i*Pr, pentyl, Bn) and the thiolato ligand. Their cytotoxicity against various human cancer cell lines of different entities reached IC_{50} values in the single-digit micromolar range. The complexes were also assayed for the induction of tumour cell apoptosis (activation of caspase-3/7), TrxR inhibition and antiangiogenic effects in zebrafish. Cyclopropene-bearing congeners were employed in click reactions to examine the subcellular accumulation of the complexes.

Introduction

In 2022, *Hanahan* et al. published another update on their cancer hallmarks, underlining the disease's complexity.[1] This update also shows which targets cancer cells, as opposed to nonmalignant cells, might offer for chemotherapy. Approved metallodrugs such as cisplatin draw what little selectivity they have for cancer cells only from their higher proliferation rate. Alternatives that address tumour-only targets would be less likely to cause unwanted side effects and drug resistance, the main problems which hamper the efficacy of platinum drugs.[2] Two cancer-specific hallmarks are the alteration of the cancer cells' metabolism and tumour (neo)vascularisation. The irregular microcirculation and diffusion conditions in solid tumours lead to hypoxic areas and, eventually, a necrotic core.[3] The subsequent switch to an anaerobic metabolism occurs by expressing transcription genes like HIF-1α. Given that chronic hypoxia is a unique feature of malignant cells, the inhibition of HIF-1α represents an interesting and selective therapeutic approach.[4] Besides the well know HIF-1α inhibitor YC-1 (*Lificiguat*),[5] adamantyl-bearing drugs, namely nicotinic or isonicotinic ester derivates and a morpholine-substituted analogue stood out in a chemical library screening.[6] Arising particularly promising from this HRE-dependent, cell-based assay was methyl 2-(4-adamantan-1-yl-phenoxymethyl)-1H-benzimidazole-5-carboxylate (**AC1-004**). The compound showed low single-digit micromolar GI_{50} values against various human cancer cell lines. The *in vivo* studies were particularly striking, showing that tumour growth in mice could be reduced by up to 59%.[7] Our current study aimed to enhance the drug's effects using the so-called metal drug synergism. The coordination of an already active compound as a ligand to a metal fragment frequently leads to complexes of higher selectivity, a lower risk of unwanted side effects and a higher retention time due to their greater stability.[8] Via *N*,*N*′-dialkylation the 5-carboalkoxybenzimidazole moiety of **AC1-004** can be transformed into an NHC ligand. By simultaneously replacing the 4-(adamant-1-yl) phenyl ether by the corresponding thiol as the second ligand incorporating the Au–S–R motif of auranofin, which was proved

[a] *S. W. Schleser,[+] L. H. F. Köhler,[+] F. Riethmüller, S. Reich, L. Schlotte, J. Seib, Prof. Dr. R. Schobert*
Chair of Organic Chemistry I
University of Bayreuth
Universitätsstraße 30
95440 Bayreuth (Germany)
E-mail: rainer.schobert@uni-bayreuth.de
[b] *R. Fertig, A. Goller, Prof. Dr. R. Kempe*
Chair of Inorganic Chemistry II
University of Bayreuth
Universitätsstraße 30
95440 Bayreuth (Germany)
[c] *Prof. Dr. G. Begemann*
Developmental Biology
University of Bayreuth
Universitätsstraße 30
95440 Bayreuth (Germany)
[+] *These authors contributed equally to this work*

Supporting information for this article is available on the WWW under https://doi.org/10.1002/cplu.202300167

Part of a Special Collection on Gold Chemistry

to be highly effective in preclinical studies,[9] we expected to achieve accompanying anti-tumour effects such as inhibition of TrxR and an increase in ROS.[10] The literature bristles with examples of NHC-gold complexes with very different mechanisms of action depending on their ligands.[11] Despite the broad portfolio of known NHC-gold complexes, there is no rational approach to combining conducive 'metal effects' with those of intrinsically bioactive ligands. We now synthesised twelve new NHC gold(I) chlorido and thiolato complexes structurally akin to HIF-1α inhibitor **AC1-004** and investigated their stability, cytotoxicity, and mode of action, depending on the substituents of the organic ligand. The subcellular accumulation of the complexes was traced by copper-free bioorthogonal click chemistry.

Results and Discussion

Synthesis and characterisation

The novel ligand 4-(adamantan-2-yl)benzenethiol (**4**) was synthesised in three steps with an overall yield of 53% (Scheme 1). Benzene was *Friedel-Crafts* alkylated with 2-bromoadamantane (**1**) affording 2-phenyladamantane (**2**) with 84% yield, which was used without further purification. Chlorosulfonation led, nearly quantitatively, to 4-(adamantan-2-yl)benzenesulfonyl chloride (**3**), which, again without further purification, was reduced to the desired 4-(adamantan-2-yl) benzenethiol (**4**) with a yield of 64%.[12]

The reference, methyl 2-(4-adamant-1-yl-phenoxymethyl)-1H-benzimidazole-5-carboxylate (**AC1-004**), was synthesised as described in the literature (Scheme 1).[7] The synthesis of 5-methoxycarbonyl-1,3-dialkylbenzimidazolium halides **7a**–**e** followed our established procedure (Scheme 1).[20] Their subse-

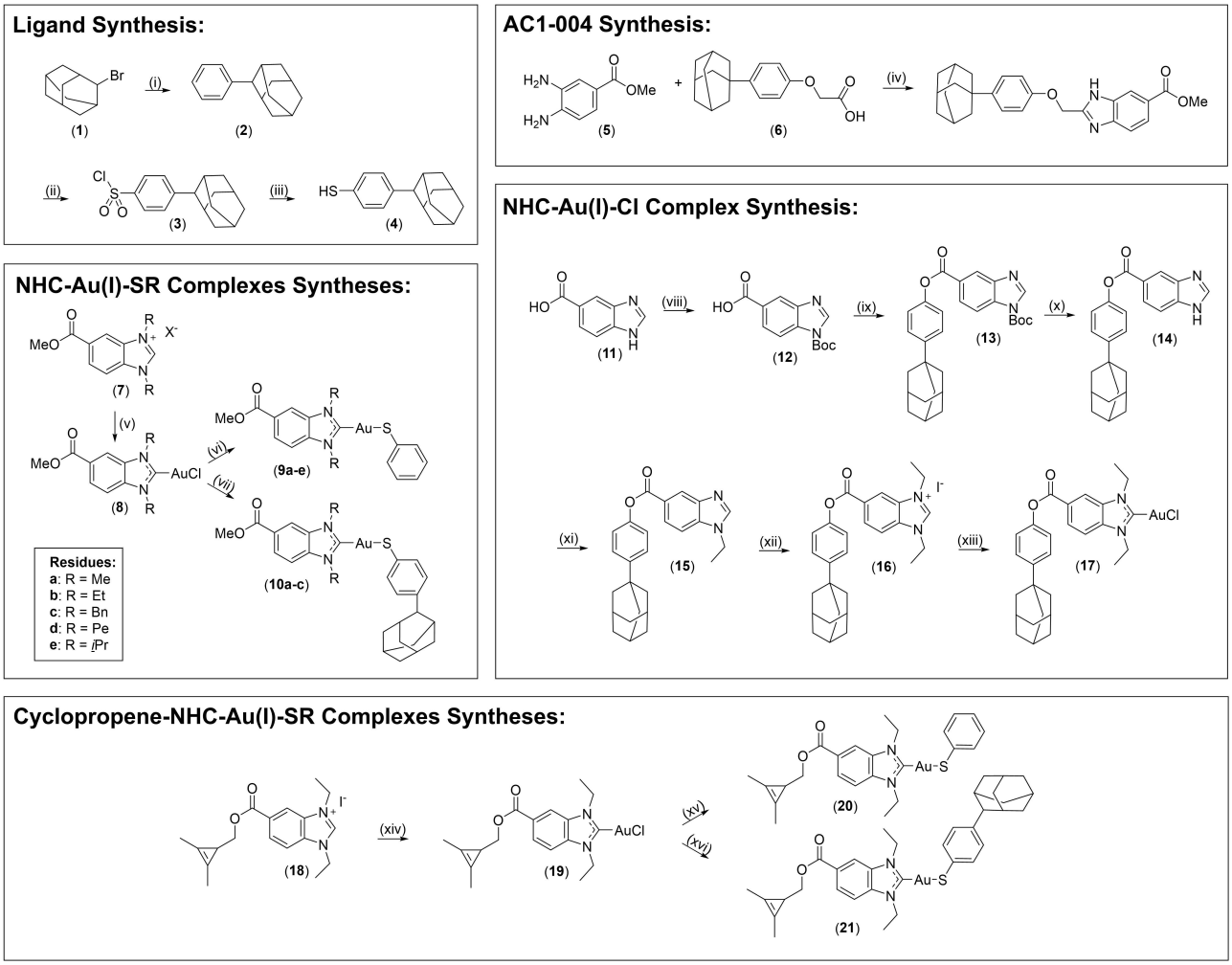

Scheme 1. Reagents and conditions: (i) $FeBr_3$, PhH, 0 °C–>80 °C, 48 h, 84%; (ii) H_3SOCl, CH_2Cl_2, 0 °C–>45 °C, 4.5 h, 98%; (iii) Me_2SiCl_2, Zn, DMAC, DCE, 75 °C, 1 h, 64%; (iv) PPSE, 140 °C, 4 h, 89%; (v) 1. Ag_2O, CH_2Cl_2, light exclusion, r.t., 6 h; 2. $AuCl(SMe_2)$, CH_2Cl_2, light exclusion, r.t., 24 h; (vi) Na, HSPh, MeOH, r.t., 24 h; (vii) KO^{t}Bu, **4**, CH_2Cl_2, r.t., 24 h; Boc_2O, 10% $Na_2CO_{3(aq.)}$, 1,4-dioxane, r.t., 16 h, 80%; (ix) EDC·HCl, DMAP, 4-(1-adamantyl)(C_6H_4)OH, CH_2Cl_2, r.t., 24 h, 84%; (x) TFA, CH_2Cl_2, r.t., 4 h, quant.; (xi) EtI, K_2CO_3, DMF, 50 °C, 24 h, 80%; (xii) EtI, 1,4-dioxane, reflux, 24 h, quant.; (xiii) 1. Ag_2O, CH_2Cl_2, light exclusion, r.t., 6 h; 2. $AuCl(SMe_2)$, CH_2Cl_2, light exclusion, r.t., 24 h, 66%; (xiv) 1. Ag_2O, CH_2Cl_2, light exclusion, r.t., 6 h; 2. $AuCl(SMe_2)$, CH_2Cl_2, light exclusion, r.t., 24 h, 74%; (xv) KO^{t}Bu, HSPh, CH_2Cl_2, r.t., 24 h, 82%; (xvi) KO^{t}Bu, **4**, CH_2Cl_2, r.t., 24 h, 72%.

quent complexation and transmetalation proceeded well and reproducibly for all salts, with hardly any noticeable influence of the N-substituents on the yield of the complexation. The final exchange of the chlorido for a thiophenol ligand in complex **8** was carried out in methanol with *in situ* generated NaOMe to afford thiophenol complexes **9**. However, this method could not be applied for an exchange of chlorido for thiol **4** because of the insolubility of the latter in methanol. Changing the solvent to CH_2Cl_2 and the base to KO^{t}Bu eventually gave the desired thiol complexes **10a–c**. The isopropyl and pentyl analogues **10d** and **10e** could not be obtained in this way, despite variations of the reaction conditions.

Crystals of **9b** suitable for X-ray diffraction analyses were grown by slow evaporation of a saturated solution in CH_2Cl_2/*n*-hexane. Figure 1 shows the resulting molecular structure. The length of the Au–S bond is longer than an average Au–S bond, nicely visualising the *trans* effect of the NHC ligand.[13] Both ligands, thiophenol and NHC, are arranged near-linearly with a C–Au–S bond angle of 177.76°.

To further determine the influence of the thiol ligands on the cytotoxicity of the compounds, the gold chlorido complex **17** was synthesised. This connects the 4-adamantylphenyl motif of **AC1-004** with the benzimidazolium NHC ligand via an ester bond (Scheme 1). Moreover, as our group has found in previous studies that the target of certain gold(I) NHC-complexes depended on their second ligand,[8a] with chlorido ligands directing them towards cell nuclei, the evaluation of complex **17** should provide insight into the influence of the thiol ligands of complexes **9** and **10** on their overall cytotoxicity mechanism of action. Protection of the amine group was necessary to achieve the esterification of benzimidazole carboxylic acid **11** with sterically more demanding alcohols like phenols. Boc was chosen for its acid lability since the ester proved relatively labile in upcoming steps. After a *Steglich-Hassner* esterification of protected benzimidazole **12** and subsequent deprotection of product ester **13**, the N-alkylation of benzimidazole **14** had to be conducted in two steps. Direct N,N′-dialkylation attempts resulted in poor yields mainly because of saponification of the ester functionality. Under milder conditions, compound **14** was monoalkylated by ethyl iodide/potassium carbonate to afford **15** in 80% yield and high purity. Without any base present, the ethylation of **15** afforded iodide **16** quantitively. As usual, the latter was converted to the gold complex **17** in 66% yield via the silver complex, just like the methyl esters. It is worth noting that attempts to react iodide **16** with Ag_2O followed by half an equivalent of $AuCl(SMe_2)$ in $MeOH/CH_2Cl_2$ to generate the cationic $[(NHC)_2Au^+]BF_4^-$ complex failed, leading instead to the bis[5-(methoxycarbonyl)-(N,N′-diethyl)benzimidazol-2-ylidene]Au$^+$ complex and recovered 4-(1-adamantyl)phenol. Dry methanol and the intermediate AgOH were nucleophilic and basic enough to cleave the labile, sterically crowded phenol ester. Repeating the reaction in dry CH_2Cl_2 resulted in saponification.

The ethyl-substituted complexes of the respective series **9b**, **10b** and **17** were subjected to stability studies. None of the complexes showed a change of their signals in ^{1}H NMR spectra over at least three days when dissolved in DMSO-d_6 + 5% D_2O, i.e. under biotest-like aqueous conditions. Hence, they can be considered stable under conditions applied in the bio-evaluation assays. The complexes were even found to be fairly stable in aqueous solution in the presence of a large excess of sodium acetylcysteine,[22] although a decrease of the adsorption intensity in respective UV/Vis spectra due to turbidity indicates some decay. In ^{1}H-NMR stability studies, no precipitation was observed upon adding D_2O. Notably, even complex **17**, a gold chlorido complex, which are normally most susceptible to ligand exchange with thiols, remained stable in an aqueous solution for several days. This finding confirms that ligand exchange with thiols did not occur and helps to explain why **17** did not show any ROS activation. (Figure 2).

To determine the subcellular accumulation and so obtain an indication of the mechanism of antitumoural action, cyclopropene analogues of complexes **9b** and **10b** were synthesised (Scheme 1). This moiety allows visualisation of the compound via a ring strain promoted *Diels Alder*$_{(inv.)}$ domino reaction with fluorescent tetrazine dyes while retaining a high structural similarity to the corresponding methyl esters. We recently published the synthesis of the benzimidazolium precursor.[14] Its complexation to give gold complex **19** via a silver complex and its transmetalation with $AuCl(SMe_2)$ proceeded analogously to synthesising complexes **8** and **17**. Likewise, the exchange of the chlorido ligand of **19** for the respective thiol afforded the complexes **20** and **21** with 70% yield.

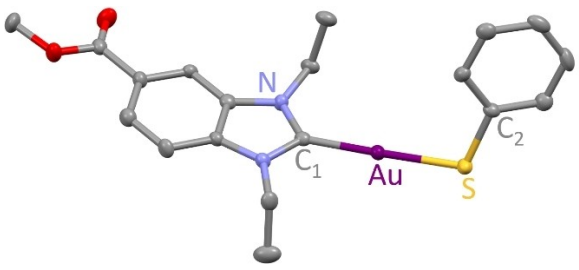

Figure 1. Molecular structure of complex **9b** as thermal ellipsoid representations at the 50% probability level (H atoms omitted). Selected bond lengths [Å] and angles [°]: C_1–Au 1.990, Au–S 2.292, Au–S–C_2 106.09, C_1–Au–S 177.76.

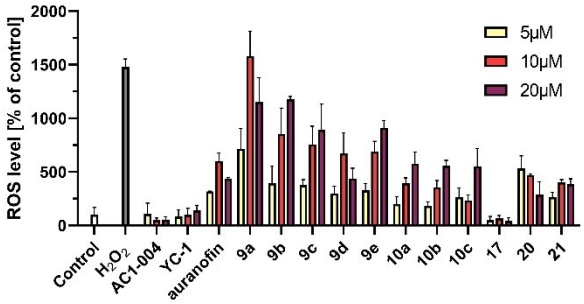

Figure 2. Fluorescence-based DCFH-DA assays showed the reactive oxygen species (ROS) levels in 518A2 melanoma cells treated with 5, 10 and 20 µM of test compounds **9a–e**, **10a–c**, **17**, **20**, **21**, **AC1-004**, YC-1, auranofin and the positive control hydrogen peroxide (H_2O_2, 1 µM) compared with solvent treated cells set to 100%. The values are means ± SD from at least three independent experiments.

It should be noted, that for technical reasons no elemental analyses could be obtained for compounds **9a**,**d** and **10b**,**c** and only analyses with C-values beyond tolerance for compounds **9c**,**e** and **21**. Since their identity and purity was confirmed by UPLC-HRMS and NMR spectra, they were provisorily included in the bioevaluation assays.

Biological evaluation

Inhibitory effect on cancer cell proliferation

The antiproliferative activity of the complexes **9a**–**e**, **10a**–**c**, **17**, **20**, **21** and of the positive controls **AC1-004**, YC-1, and auranofin was tested via MTT assays. Eight cancer or hybrid cell lines of six entities were treated for 72 h, and IC_{50} values were calculated using GraphPad Prism 9 (Table 1). The thiophenol Au(I) complexes **9** with mainly single-digit micromolar IC_{50} values were more active than the 4-(adamantan-2-yl)benzenethiolato Au(I) complexes **10**, which featured IC_{50} values predominantly in the double-digit micromolar range. The IC_{50} values of the thiophenolato Au(I) complex with a cyclopropene moiety **20** were lower on average than those of its bulkier analogue **21**, comparable to or lower than those of its methyl ester analogue **9b**. Within series **9** (thiophenolato), there was a slight increase in activity with increasing N-substituent lipophilicity. The opposite effect was found for complexes **10**, whose activities declined with increasing residue size, possibly due to an associated decrease in solubility. The cells were also treated with lead compound **AC1-004**[7] (15.4 μM), the known HIF-1α inhibitor YC-1[5] (17.7 μM) and auranofin[15] (3.6 μM) for comparison. Cell line-specific effects were observed for the multi-drug resistant KB–V1 cervix carcinoma cell line, which was sensitive to **9a**, **AC1-004** and auranofin.[16] Some cell lines showed compound-specific resistance within the concentration range tested (100 μM–0.5 nm) with IC_{50} values above 50 μM.

These included 518A2 melanoma cells (**10c** and **17**), EA.hy926 endothelial hybrid cells (YC-1, **10c** and **17**), U87 glioblastoma cells (YC-1) or HCT116 colon carcinoma cells (**17**). HCT116 cells lacking functional p53 were more sensitive to most test compounds than the wild type with functional p53. A few selected compounds (**9b**, **10b**, **17** and **20**) as well as **AC1-004** and auranofin were tested on nonmalignant human dermal fibroblasts (HDFa) to investigate their selectivity for cancer cells. **AC1-004** and **9b** were highly selective for cancer cells compared to chlorido complex **17**, cyclopropene analog **20**, adamantyl derivative **10b** and auranofin.

Impact on the cellular redox system

Substance-induced toxicity in cancer cells can originate from oxidative stress due to an elevated reactive oxygen species (ROS) level.[17] This often leads to cell cycle arrest, senescence or cell death and counteracts the tumour-promoting effects of ROS in many cancer types.[18] Intracellular formation of ROS can be quantified by 2',7'-dichlorodihydrofluorescein diacetate (DCFH-DA), which is converted to DCFH by cellular esterases and turns fluorescent when oxidised by intracellular ROS.[19] Gold(I) complexes like auranofin might induce ROS formation by interacting with thiol-containing enzymes like thioredoxin reductase (TrxR).[20] The measurement of ROS in 518A2 melanoma cells after treatment with 5 μM of test compounds **9a**–**e**, **10a**–**c**, **17**, **20**, **21** and with the controls **AC1-004**, YC-1, and auranofin showed a distinct increase for all Au(I) complexes (Figure 2). An exception was chlorido complex **17**, which, like **AC1-004** and YC-1, induced no ROS increase. Once more, complexes **9** showed ascending activities from **9e** to **9a**. Moderate ROS inductions were observed for complexes **10** and the cyclopropenyl derivatives **20** and **21**. The Au(I)-thiolato motif, which the lead structure **AC1-004** lacks, is essential for a distinct ROS induction. Complexes **9a**–**c** and **10a**–**c** also inhibited the activity of TrxR, as was previously shown for auranofin (Figure S64, Supporting Information), suggesting a similar mechanism through a deficient control of oxidative stress and redox regulation.[21]

Table 1. Mean IC_{50} values ± SD [μM] of test compounds **9a**–**e**, **10a**–**c**, **17**, **20**–**21**, **AC1-004**, YC-1, and auranofin against 518A2 melanoma, EA.hy926 endothelial hybrid, U-87 glioblastoma, MCF-7 breast carcinoma, HT-29 colorectal adenocarcinoma, KB–$V1^{Vbl.}$ cervix carcinoma, HCT116 wildtype and p53 knockout colon carcinoma cells and adult human dermal fibroblasts (HDFa) after 72 h.

	IC_{50} (72 h) [μM] 518A2	EA.hy926	U-87	MCF-7	HT-29	KB-$V1^{Vbl.}$	Hct116	Hct116p53	mean IC_{50}	HDFa
AC1-004	17.3 ± 1.7	5.7 ± 0.4	45 ± 0.6	12.5 ± 1.1	17.9 ± 1.5	1.4 ± 0.2	11.4 ± 2.0	12.3 ± 0.6	15.4	> 50
YC-1	0.9 ± 0.04	> 50	> 50	5.1 ± 0.3	1.2 ± 0.1	21.6 ± 5.3	0.8 ± 0.1	12.3 ± 0.6	17.7	–
auranofin	1.6 ± 0.1	5.2 ± 0.2	4.6 ± 0.1	4.5 ± 0.09	5.0 ± 0.1	3.4 ± 0.4	2.4 ± 0.2	2.2 ± 0.3	3.6	6.4 ± 0.7
9a	15.6 ± 0.8	4.1 ± 0.4	3.7 ± 0.08	4.2 ± 0.5	14.5 ± 0.6	4.8 ± 0.5	16.5 ± 1.1	10.6 ± 1.5	9.3	–
9b	18.8 ± 1.3	6.8 ± 0.7	5.7 ± 1.0	14.0 ± 0.5	11.8 ± 1.3	18.8 ± 1.2	11.6 ± 0.8	5.9 ± 0.1	11.7	39.6 ± 1.2
9c	20.7 ± 1.0	2.1 ± 0.2	2.8 ± 0.2	2.5 ± 0.3	5.4 ± 0.2	10.6 ± 1.1	12.8 ± 1.8	5.3 ± 0.2	7.8	–
9d	7 ± 0.2	5.5 ± 0.3	7.2 ± 0.2	8.1 ± 0.1	16.6 ± 0.6	15.7 ± 1.2	7.2 ± 0.5	2.3 ± 0.3	8.7	–
9e	6.1 ± 0.4	9.7 ± 0.7	2.0 ± 0.04	4.0 ± 0.04	6.6 ± 0.6	14.2 ± 0.5	5.2 ± 0.2	3.6 ± 0.4	6.4	–
10a	17.8 ± 1.4	15.7 ± 1.5	20.6 ± 2.0	14.4 ± 1.6	19.8 ± 1.2	27.1 ± 1.1	17.0 ± 0.9	13.8 ± 0.9	18.3	–
10b	17.2 ± 1.3	17.2 ± 1.2	33.4 ± 1.1	12.7 ± 0.8	29.2 ± 2.2	39.6 ± 4.5	8.5 ± 0.8	7.1 ± 0.5	20.6	18.4 ± 2.1
10c	> 50	> 50	35.1 ± 0.8	23.8 ± 2.0	25.3 ± 1.8	> 50	42.0 ± 2.2	8.7 ± 0.6	35.6	–
17	> 50	> 50	19.2 ± 2	8.6 ± 1.5	7.0 ± 0.7	32.0 ± 2.2	> 50	42.2 ± 0.3	32.4	> 50
20	5.2 ± 0.04	5.5 ± 0.2	6.7 ± 0.3	7.8 ± 0.4	15.6 ± 1.2	16.4 ± 1.7	7.0 ± 0.4	5.9 ± 0.1	8.8	18.7 ± 1.8
21	9.3 ± 0.7	11.4 ± 1.0	36.3 ± 0.8	22.9 ± 4.4	43.3 ± 6.2	20.3 ± 2.5	17.7 ± 3.0	11.6 ± 1.0	33.3	–

Interference with the cancer cell cycle

A common downstream effect of increased ROS levels and TrxR inhibition is altering the number of cells in the different cell cycle phases. We analysed such potential effects by the new complexes on 518A2 melanoma cells using fluorescence-assisted cell sorting (FACS) (Figure 3). In contrast to compounds **AC1-004**, **9b**, **10a**, **10c**, and **17**, which showed no change in cell cycle distributions, the complexes **9a**, **9c**–**e**, **10b**, compound YC-1, and especially auranofin induced an increase in the sub-G1 cell population, which is indicative of apoptosis, and subsequently led to a decrease in G1-phase cells. The investigation of cell death using a caspase 3/7 assay kit revealed a significant increase in activity for **9d** and the positive control staurosporine (STA) after incubation for 6 h (Figure S65, Supporting Information). This suggests an apoptotic pathway for **9d**, which also caused a notable S-phase arrest in 518A2 cells.

Since S-phase arrest is usually associated with disruption of DNA replication or impairment of CDK (cyclin-dependent kinases)-controlled cell cycle checkpoints, a possible interaction with DNA was investigated via electrophoretic mobility shift assays (EMSA), which revealed no interaction of **9d** with ds-DNA (Figure S66, Supporting Information).[22] A slight increase in G2/M-phase cells for **9c**–**e** was observed.

Reorganisation of the actin cytoskeleton

Cell apoptosis and oxidative stress are frequently associated with the dynamics of the actin cytoskeleton.[23]

A considerable body of evidence suggests a close relationship between the actin cytoskeleton and the regulation of mitochondrial function as a possible point of apoptotic regulation in eukaryotic cells.[24] Fluorescence microscopy images of 518A2 cells after treatment with complexes **9a**–**c**, **10a**–**c**, **17** (10 μM), **9d**–**e** (5 μM) and auranofin (1 μM) revealed a concentration-dependent remodelling of the actin cytoskeleton (Figure 4). The concentrations of auranofin and complexes **9d** and **9e** were reduced to 1 and 5 μM, respectively, due to their stronger cytotoxic effects on the cells. Reorganisation of the actin cytoskeleton resulted in alterations such as stress fibre formation, actin degradation and clustering. The integrity of cells was also affected, resulting in the detachment of focal adhesions and rounded cell morphology.[25] Since apoptosis is characterised by nuclear fragmentation in most cell types, either no apoptosis has been induced, or an early stage has not yet led to nuclear degradation.[26] In contrast, **AC1-004** and the HIF-1α -inhibitor YC-1 (10 μM) showed no effects on the actin filaments, indicating that it might be the gold complex fragment responsible for the effects on the actin cytoskeleton.

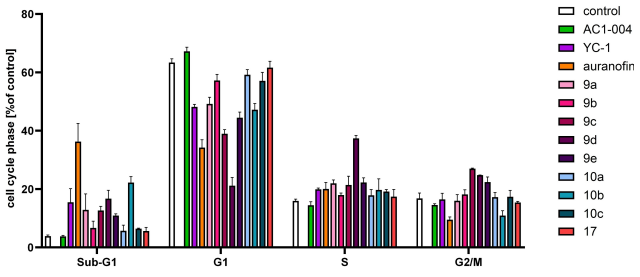

Figure 3. Effect of compounds **9a**–**e**, **10a**–**c**, **17**, **AC1-004**, YC-1, (10 μM) and auranofin (5 μM) on the cell distributions in the different cell cycle phases of 518A2 melanoma cells after 24 h of treatment. Values ± SD of two independent experiments were derived from at least 10000 counted cells with solvent-treated control set to 100%.

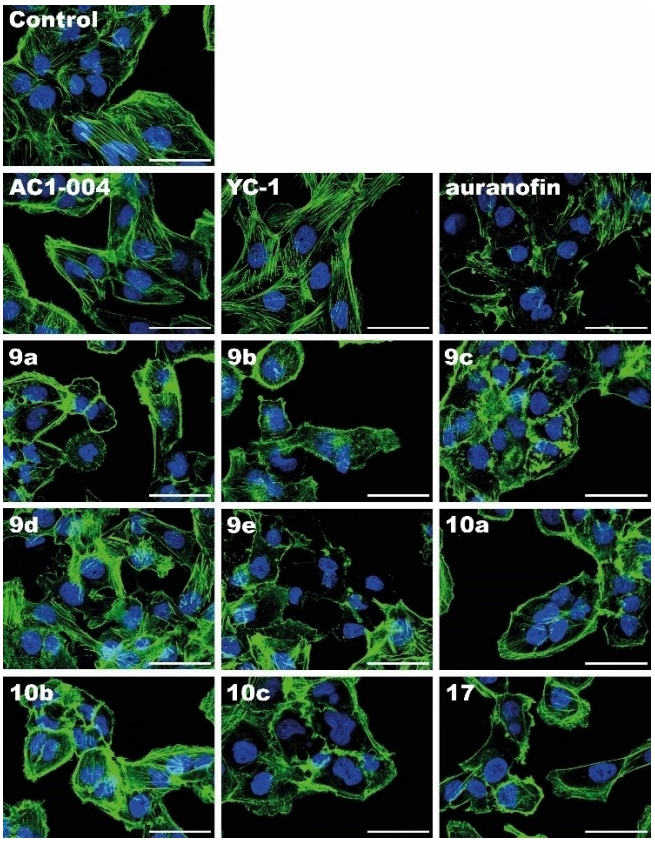

Figure 4. Immunofluorescence images of the actin cytoskeleton (green) and the nuclei (blue) of 518A2 melanoma cells after treatment with compounds **9a**–**c**, **10a**–**c**, **17**, **AC1-004**, YC-1, (10 μM), **9d**–**e** (5 μM) or auranofin (1 μM) for 24 h. Images are representative of at least two independent experiments. Scale bars correspond to 50 μm, magnification 640×.

Subcellular localisation

The similarity of the cyclopropene derivatives **20**, **21** and their counterparts **9b** and **10b** in terms of their effects in the MTT and DCFH-DA ROS formation assays suggest a related mode of action, very likely also involving similar targets and sites of accumulation in the cells. This justifies using compounds **20** and **21**, which can be fluorescently labelled by a *Diels-Alder* reaction,[27] as a probe for identifying not just their site of intracellular localisation but that of **9b** and **10b** as well. Figure 5 shows the subcellular distribution of the fluorescent click-products of complexes **20** and **21** in 518A2 cells with counterstained nuclei and mitochondria.

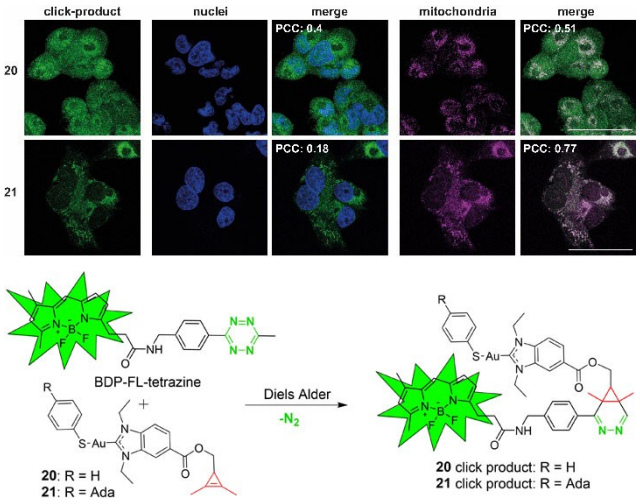

Figure 5. Confocal imaging of 518A2 melanoma cells treated with 25 μM of cyclopropene derivatives **20** or **21** and BDP-FL-tetrazine for bioorthogonal labelling (green), or with MitoTracker® Red CM-H2XRos (violet), or DAPI (blue). Images are representative of at least two independent experiments. Scale bars correspond to 50 μm, magnification 640×. Pearson correlation coefficient (PCC) was calculated for colocalised nuclei and mitochondria using the coloc2 function (image J). The bottom scheme shows the general cycloaddition reaction of cyclopropenes **20** and **21** with BPD-FL-tetrazine to give fluorescent diazines.

Surprisingly, the adamantyl group of complex **21** affected the distribution within the cell, resulting in a selective accumulation within mitochondria. In contrast, complex **20** was detected in mitochondria, nuclei, and cytoplasm, indicating a rather unspecific distribution. Pearsons correlation coefficient (PCC) was used to quantify the accumulation within the cell organelles, with values near 1 standing for a complete overlay of both images. Mitochondria, which play a major role in crucial metabolic functions of the cell and the regulation of apoptosis, and cancer-specific phenomena such as the overproduction of ROS, are an important target for cancer treatment.[28] When we assume similar mitochondrial mechanisms of action for **20**/**21** and **9b**/**10b**, the latter will likely operate by induction of ROS-induced cancer cell death.[29] To further substantiate the comparability of complexes **9**, **10**, and **17**, their uptake into 518A2 cells was quantified by ICP-MS analysis, yielding values between 8 and 19 ng of gold per $1*10^6$ cells for compounds **9a**–**e**, **10b** and **17** (Figure S67, Supporting Information). In comparison, the uptake of auranofin was 13-fold higher with 255 ng, which constitutes a significantly poorer uptake of the test substances.

Influence on endothelial tube formation

Another consequence of elevated oxidative stress in cancer cells is the upregulation of proliferation-enhancing transcription factors such as NF-κB, VEGF or HIF-1α, which are responsible for tumour growth, migration, invasion or the induction of angiogenesis.[30] The development of new blood vessels promotes the growth of tumours and increases the risk of metastasis.[31] The investigation of agents that inhibit angiogenesis in tumour tissue constituted a key point in developing new cancer therapies.[32] The anti-angiogenic potential of the test compounds **9a**–**e**, **10a**–**c**, **17**, **AC1-004**, YC-1, and auranofin (20 μM) was examined by their inhibitory effects on the *in vitro* formation of vessel-like tubes by EA.hy926 endothelial hybrid cells (Figure S68, Supporting Information).[33] Growing these cells on a solubilised basement membrane matrix for 10 h led to the formation of polygonal tubes mimicking 2D vessel-like structures in the solvent-treated wells. Upon addition of the test compounds, different changes in the extent of tube formation were observed. Auranofin had the strongest inhibitory effect, apparent from suppressing tubular structure formation and a substantial reduction of cell vitality as determined by concomitant MTT assays. Complexes **9** and **10b** also showed distinct inhibitory effects on the migration of cells and the formation of cell-cell junctions, leaving merely small contiguous cell clusters and isolated tubes aside from individual cells. **10a**, **10b**, **17**, **AC1-004** and YC-1 led to the formation of polygonal structures similar to solvent-treated cells, not indicating any noteworthy anti-angiogenic effect.

Anti-angiogenic effect on zebrafish larvae

To confirm the anti-angiogenic properties *in vivo* and to investigate possible toxic effects in a vertebrate model, the angiogenesis of zebrafish larvae (24 hpf, hours post fertilisation) was investigated under compound exposure. Initially, the larvae showed a concentration-dependent tolerance for the test substances, so the concentrations vary between 1 and 10 μM (Figure 6). While compounds **9a, 9b**, **9e**, **AC1-004** and auranofin were tolerated up to a maximum concentration of only 1 μM, complex **9d** was tolerated with a maximum concentration of 5 μM, and compounds **9c**, **10a**–**c**, **17**, and YC-1 even at 10 μM. The 4-(adamantan-2-yl)benzenethiolato

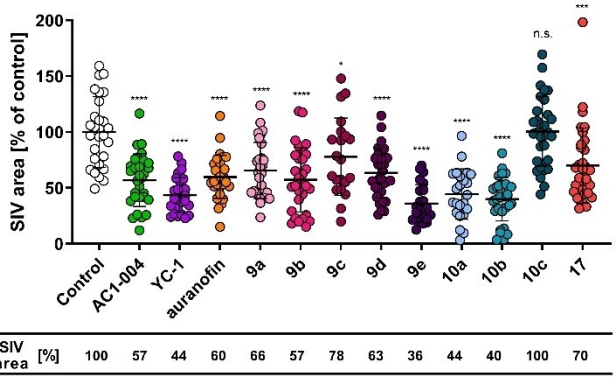

Figure 6. At least 21 zebrafish larvae each were treated with test compounds **9c**, **10a**–**c**, **17**, YC-1 (10 μM), **9d** (5 μM), **9a**, **9b**, **9e**, **AC1-004** and auranofin (1 μM) for 48 h. To estimate the antiangiogenic effect, the SIV (subintestinal vessel) area was quantified via ImageJ and quoted as the mean ± SD with solvent-treated fish set to 100%. Significance is given as n.s.: > 0.05; *: < 0.05; ***: < 0.001; ****: < 0.0001, One-way ANOVA with Dunnett's multiple comparison test (GraphPad Prism 9).

complexes and YC-1 and **9c** showed significantly fewer toxic effects than **AC1-004**, auranofin, and three of the thiophenolato complexes, with **9d** lying in between. Considering the effect on the formation of the subintestinal vein (SIV) in zebrafish larvae, an impairment of angiogenesis was observed for all test compounds except **10c**. A benzyl group reduced the activity on the NHC ligand (**9c** and **10c**) and for the chlorido complex **17**.

The strongest anti-angiogenic effect was exhibited by **9e**, **10a**, **10b** and YC-1, which is known to inhibit HIF-1α and VEGF.[34] When applied at a concentration of only 1 μM, **9e** was the most intrinsically active angiogenesis inhibitor.

Conclusion

The aim of this study was the synthesis and biological evaluation of NHC gold complexes that are structurally similar to **AC1-004** and potentially combine the anticancer effects with the known antioxidant properties of gold complexes.[35] The crystal structure of **9b** confirmed the linear geometry of the gold(I) coordination and the *trans* influence of the NHC ligand through a noticeably lengthened Au–S bond length. The stability of the complexes in an aqueous milieu and with free thiols present over a few days was confirmed for one representative of each series, i.e. **9b**, **10b** and **17**. The efficacy of the new test complexes against human cancer cell lines in terms of IC_{50} values in MTT assays spanned a wide range from 2.1 to >50 μM, depending on the substituents of the NHC ligand, as well as on the nature of the thiolato ligand. Longer and branched alkyl substituents (**9d–e**) improved the efficacy, whereas benzyl groups led to a loss of efficacy (**9c**, **10c**). The 4-(adamant-2-yl)phenyl moiety (**10a–c**, **17**, **21**), which is reportedly responsible for the destabilisation of HIF-1α by **AC1-004**, led to a lower efficacy. Cytotoxicity studies against nonmalignant HDFa cells demonstrated the selectivity of thiophenyl derivative **9b** and the lead compound **AC1-004** for cancer cells. The best-performing complexes of our small library keep abreast of the front line of known anti-tumoural NHC Au(I) complexes.[36] Like for most of the latter, the redox properties of our complexes play a significant role in their effect. For the influence on the cellular ROS levels, there is a clear SAR. Thiophenolato complexes **9** induced higher ROS levels than their respective 4-(adamant-2-yl)thiophenolato analogues **10** with identical N-residues. Likewise, ROS induction grew in series **9** and **10** when going from bulkier to smaller N-residues. The inhibition of tumoral TrxRs by complexes **9** and **10** was found causative for the increased ROS levels in treated tumour cells. In line with this finding, the cyclopropene derivatives **20** and **21** accumulated in the mitochondria of melanoma cells which are mainly responsible for the cell's redox metabolism and proliferation signalling.[37] Some of the test compounds influenced the distribution of cells in the different phases of the cell cycle. A clear SAR could not be identified, but **9d** stood out with a distinct S-phase arrest and caspase 3/7 induction. However, any direct interaction with DNA, which is a major cause of S-phase arrest, could be ruled out by EMSA.[38] The observed alteration of actin filaments in treated cells might be linked to the overproduction of mitochondrial ROS and TrxR inhibition, leading to an aberrant motility, shape, and membrane integrity of the cells and eventual cell death.[24] The degradation of the actin cytoskeleton caused by **9d**, **9e** and auranofin could indicate ongoing apoptosis associated with degradation by caspases.[39] It is not clear whether the strong anti-angiogenic effects observed for gold complexes **9a–e** and **10b**, compared to controls YC-1 and **AC1-004**, in the tube-formation assay are due to degradation of the actin cytoskeleton or inhibition of the Akt signalling pathway as is the case for **AC1-004** and a resulting HIF-1α-destabilisation.[7] The strong anti-angiogenic potential of the test compounds was confirmed by the reduction of blood vessel development in zebrafish.[40] In summary, unlike **AC1-004**, on which they were modelled, some new complexes exhibited distinct pleiotropic effects on cancer cells, such as ROS increase, cell cycle alteration, actin reorganisation, and restricted angiogenesis. Whether the latter is possibly associated with HIF-1α inhibition needs to be ascertained in follow-up studies. We found that thiophenolato complexes with large N-substituents were more efficacious. In contrast, the 4-(adamant-2-yl)benzenethiolato derivatives with small alkyl substituents accumulated more selectively in the mitochondria and were better tolerated in the zebrafish model. This tentative SAR should now enable a more rational optimisation of this compound class, e.g. by starting with **9e**, the most promising complex of the current study.

Experimental Section

General procedure for the synthesis of thiophenolato complexes 9

Sodium (2.00 eq.) was dissolved in dry MeOH (200 mL/mmol). The resulting solution of sodium methoxide was treated with thiophenol (1.00 eq.) and stirred for 1 h at rt. The respective gold chlorido complex **8** (1.00 eq.) was added portionwise to the now yellow solution of sodium thiophenolate. After stirring at rt for 24 h, the solvent was evaporated, and the remainder was suspended in CH_2Cl_2 and filtered. The filtrate was concentrated in vacuo, and the residue was precipitated in pentane. The thiophenolato complexes **9** were isolated as yellowish powders after filtration and drying *in vacuo*.

[Thiophenolato(5-methoxycarbonyl-1,3-dimethylbenzimidazol-2-ylidene)] gold(I) (9a)

17.5 mg (34.3 μmol, 68%) from sodium (2.32 mg, 100 μmol, 2.00 eq.), thiophenol (5.45 μL, 50.4 μmol, 1.00 eq.) and **8a** (22.0 mg, 50.4 μmol, 1.00 eq.) in dry MeOH (10 mL). m.p. 195 °C (decomp.); ^{1}H NMR (500 MHz, $CDCl_3$) δ_H 8.18 (s, 1H, H^{ar}), 8.16 (s, 1H, H^{ar}), 7.61 (d, J = 7.5 Hz, 2H, H^{ar}), 7.50 (d, J = 8.5 Hz, 1H, H^{ar}), 7.09 (t, J = 7.5 Hz, 2H, H^{ar}), 6.96 (t, J = 7.5 Hz, 1H, H^{ar}), 4.09 (s, 3H, NMe), 4.08 (s, 3H, NMe), 3.99 (s, 3H, OMe) ppm; ^{13}C NMR (125 MHz, $CDCl_3$) δ_C 192.5 (s, NCN), 166.3 (s, COOMe), 142.3 (s, C^{ar}), 136.7 (s, C^{ar}), 133.8 (s, C^{ar}), 132.6 (s, C^{ar}), 128.0 (s, C^{ar}), 126.7 (s, C^{ar}), 126.1 (s, C^{ar}), 123.2 (s, C^{ar}), 113.1 (s,

C^{ar}), 110.1 (s, C^{ar}), 52.7 (s, OMe), 35.1 (s, NMe) ppm; HRMS (ESI): m/z calculated for $C_{13}H_{15}AuN_3O$ [(NHC)Au(MeCN)]$^+$: 442.08298. Found: 442.08198; m/z calculated for $C_{22}H_{24}AuN_4O_4$ [$(NHC)_2Au$]$^+$: 605.14631. Found: 605.14561; m/z calculated for $C_{28}H_{29}Au_2N_4O_4S$ [2 M-SPh]$^+$: 911.12406. Found: 911.12265.

[Thiophenolato(5-methoxycarbonyl-1,3-diethylbenzimidazol-2-ylidene)] gold(I) (9b)

11.0 mg (20.4 μmol, 63%) from sodium (1.48 mg, 64.6 μmol, 2.00 eq.), thiophenol (3.35 μL, 32.3 μmol, 1.00 eq.) and **8b** (15.0 mg, 32.3 μmol, 1.00 eq.) in dry MeOH (5 mL). m.p. 165 °C (decomp.); ^{1}H NMR (500 MHz, $CDCl_3$) δ_H 8.20 (d, J = 1.3 Hz, 1H, H^{ar}), 8.15 (dd, J = 8.5 Hz, 1.3 Hz, 1H, H^{ar}), 7.67–7.60 (m, 2H, H^{ar}), 7.52 (d, ^3J = 8.5 Hz, 1H, H^{ar}), 7.10 (t, J = 7.7 Hz, 2H, H^{ar}), 7.01–6.92 (m, 1H, H^{ar}), 4.59 (dq, J = 9.9 Hz, 7.3 Hz, 4H, NCH_2), 3.99 (s, 3H, OMe), 1.59 (vq, J = 7.3 Hz, 6H, CH_3) ppm; ^{13}C NMR (125 MHz, $CDCl_3$) δ_C 190.9 (s, NCN), 166.4 (s, COOMe), 142.3 (s, C^{ar}), 136.0 (s, C^{ar}), 133.0 (s, C^{ar}), 132.7 (s, C^{ar}), 128.0 (s, C^{ar}), 126.6 (s, C^{ar}), 125.9 (s, C^{ar}), 123.2 (s, C^{ar}), 113.2 (s, C^{ar}), 110.1 (s, C^{ar}), 52.7 (s, OMe), 44.0 (s, NCH_2), 15.7 (s, CH_3) ppm; HRMS (ESI): m/z calculated for $C_{15}H_{19}AuN_3O_2$ [(NHC)Au(MeCN)]$^+$: 470.11428. Found: 470.11337; m/z calculated for $C_{26}H_{32}AuN_4O_4$ [$(NHC)_2Au$]$^+$: 661.20891. Found: 661.20776; m/z calculated for $C_{32}H_{37}Au_2N_4O_4S$ [2 M-SPh]$^+$: 967.18666; Found: 967.18469. Anal. Calcd. for $C_{19}H_{21}AuN_2O_2S$: C, 42.39; H, 3.93; N, 5.20, S, 5.95. Found: C, 42.77; H, 3.74; N, 5.11; S, 5.77. Crystal data: $C_{19}H_{21}AuN_2O_2S$, M = 538.41, monoclinic, space group P21/c; a = 13.180(3) Å, b = 13.170(3) Å, c = 10.710(2) Å, α = 90°, β = 101.60(3)°, γ = 90°, V = 1821.1(7) Å^3, Z = 4, λ = 0.71073 Å, μ = 8.208 mm^{-1}, T = 133 K; 28 885 reflections measured, 4398 unique; R [I > 2s(I)] = 0.0367, GOF = 1.071.

Deposition Number 2214175 contains the supplementary crystallographic data for this paper. These data are provided free of charge by the joint Cambridge Crystallographic Data Centre and Fachinformationszentrum Karlsruhe Access Structures service.

[Thiophenolato(5-methoxycarbonyl-1,3-dibenzylbenzimidazol-2-ylidene)] gold(I) (9c)

19.0 mg (28.7 μmol, 56%) from sodium (2.34 mg, 102 μmol, 2.00 eq.), thiophenol (5.20 μL, 51.0 μmol, 1.00 eq.) and **8c** (30.0 mg, 51.0 μmol, 1.00 eq.) in dry MeOH (10 mL). m.p. 165 °C (decomp.); ^{1}H NMR (500 MHz, $CDCl_3$) δ_H 8.10 (d, J = 1.3 Hz, 1H, H^{ar}), 8.01 (dd, J = 8.6 Hz, 1.4 Hz, 1H, H^{ar}), 7.54 (d, J = 7.6 Hz, 2H, H^{ar}), 7.46–7.42 (m, 2H, H^{ar}), 7.41–7.37 (m, 3H, H^{ar}), 7.36–7.32 (m, 5H, H^{ar}), 7.00 (d, J = 7.5 Hz, 2H, H^{ar}), 6.93 (t, J = 7.3 Hz, 1H, H^{ar}), 5.79 (d, J = 3.6 Hz, 4H, NCH_2), 3.91 (s, 3H, OMe) ppm; ^{13}C NMR (125 MHz, $CDCl_3$) δ_C 192.6 (s, NCN), 166.1 (s, COOMe), 142.0 (s, C^{ar}), 136.3 (s, C^{ar}), 134.4 (s, C^{ar}), 134.3 (s, C^{ar}), 133.4 (s, C^{ar}), 132.6 (s, C^{ar}), 129.2 (s, C^{ar}), 128.8 (s, C^{ar}), 127.9 (s, C^{ar}), 127.5 (s, C^{ar}), 127.4 (s, C^{ar}), 126.9 (s, C^{ar}), 126.1 (s, C^{ar}), 123.2 (s, C^{ar}), 113.9 (s, C^{ar}), 111.9 (s, C^{ar}), 52.9 (s, OMe), 52.6 (s, NCH_2) ppm; HRMS (ESI): m/z calculated for $C_{20}H_{21}AuN_3O_2$ [NHC)Au(MeCN]$^+$: 594.14558. Found: 594.14455; m/z calculated for $C_{52}H_{45}Au_2N_4O_4S$ [2 M-SPh]$^+$ 1215.24926; Found: 1215.24784; Anal. Calcd. for $C_{29}H_{25}AuN_2O_2S$: C, 52.57; H, 3.80; N, 4.23, S, 4.84. Found: C, 53.49; H, 4.26; N, 4.30; S, 4.40.

[Thiophenolato(5-methoxycarbonyl-1,3-dipentylbenzimidazol-2-ylidene)] gold(I) (9d)

27.0 mg (43.4 μmol, 92%) from sodium (2.18 mg, 94.7 μmol, 2.00 eq.), thiophenol (4.92 μL, 47.4 μmol, 1.00 eq.) and **8d** (26.0 mg, 47.4 μmol, 1.00 eq.) in dry MeOH (5 mL); m.p. 100 °C; ^{1}H NMR (500 MHz, $CDCl_3$) δ_H 8.18 (d, J = 1.3 Hz 1H, H^{ar}), 8.13 (dd, J = 8.6 Hz, 1.4 Hz, 1H, H^{ar}), 7.66–7.61 (m, 2H, H^{ar}), 7.50 (d, J = 8.5 Hz, 1H, H^{ar}), 7.09 (t, J = 7.7 Hz, 2H, H^{ar}), 7.01–6.94 (m, 1H, H^{ar}), 4.51 (dt, J = 10.3 Hz, 7.5 Hz, 4H, NCH_2), 3.99 (s, 3H, OMe), 1.97 (sext., 4H, CH_2), 1.39 (dp, J = 10.1 Hz, 3.4 Hz, 8H, CH_2), 0.89 (dt, J = 7.0 Hz, 3.8 Hz, 6H, CH_3) ppm; ^{13}C NMR (125 MHz, $CDCl_3$) δ_C 191.5 (s, NCN), 166.3 (s, COOMe), 142.4 (s, C^{ar}), 136.2 (s, C^{ar}), 133.1 (s, C^{ar}), 132.6 (s, C^{ar}), 127.9 (s, C^{ar}), 126.5 (s, C^{ar}), 125.8 (s, C^{ar}), 123.1 (s, C^{ar}), 113.4 (s, C^{ar}), 111.2 (s, C^{ar}) 52.7 (s, OMe), 49.0 (NCH_2), 30.0 (s, CH_2), 29.9 (s, CH_2), 28.9 (s, CH_2), 28.8 (s, CH_2), 22.4 (s, CH_2), 13.9 (s, CH_3) ppm; HRMS (ESI): m/z calculated for $C_{21}H_{31}AuN_3O_2$ [(NHC)Au(MeCN)]$^+$: 554.20818. Found: 554.20621; m/z calculated for $C_{44}H_{61}Au_2N_4O_4S$ [2 M-SPh]$^+$: 1135.37446. Found: 1135.37090.

[Thiophenolato(5-methoxycarbonyl-1,3-diisopropylbenzimidazol-2-ylidene)] gold(I) (9e)

30.0 mg (53.0 μmol, 65%) from sodium (3.73 mg, 162 μmol, 2.00 eq.), thiophenol (8.44 μL, 81.2 μmol, 1.00 eq.) and **8e** (40.0 mg, 81.2 μmol, 1.00 eq.) in dry MeOH (7 mL). m.p. 165 °C (decomp.); ^{1}H NMR (500 MHz, $CDCl_3$) δ_H 8.33 (d, J = 1.5 Hz, 1H, H^{ar}), 8.08 (dd, J = 8.7 Hz, 1.5 Hz, 1H, H^{ar}), 7.67 (d, J = 8.7 Hz, 1H, H^{ar}), 7.64–7.61 (m, 2H, H^{ar}), 7.10 (t, J = 7.8 Hz, 2H, H^{ar}), 7.01–6.94 (m, 1H, H^{ar}), 5.52 (dsept, J = 7.0 Hz, 5.2 Hz, 2H, NCH), 3.99 (s, 3H, OMe), 1.78 (dd, J = 13.9 Hz, 7.0 Hz, 12H, CH_3) ppm; ^{13}C NMR (125 MHz, $CDCl_3$) δ_C 189.7 (s, NCN), 166.3 (s, COOMe), 142.3 (s, C^{ar}), 135.5 (s, C^{ar}), 132.6 (s, C^{ar}), 128.0 (s, C^{ar}), 125.9 (s, C^{ar}), 125.3 (s, C^{ar}), 123.2 (s, C^{ar}), 114.7 (s, C^{ar}), 112.6 (s, C^{ar}) 54.2 (s, NCH), 54.1 (s, NCH), 52.7 (s, OMe), 22.0 (s, CH_3), 21.9 (CH_3) ppm; HRMS (ESI): m/z calculated for $C_{17}H_{23}AuN_3O_2$: 498.14458 [(NHC)Au(MeCN)]$^+$. Found: 498.14430; Anal. Calcd. for $C_{21}H_{25}AuN_2O_2S$: C, 44.53; H, 4.45; N, 4.95, S, 5.66. Found: C, 43.27; H, 4.15; N, 4.67; S, 5.36.

General procedure for the synthesis of thiolato complexes 10

The respective gold chlorido complex **8** (1.00 eq.) was dissolved in dry CH_2Cl_2 (100 mL/mmol), and KO^{t}Bu (2.00 eq.) was added. The solution was left stirring for 1 h at rt and then treated in portions with 4-(adamantan-2-yl)benzenethiol (**4**) (1.00 eq.). After stirring at rt for 24 h, the suspension was filtered over Celite, and the filtrate was evaporated to dryness. The remainder was precipitated in pentane to afford the target complexes **10** as yellowish powders after filtration and drying *in vacuo*.

[(4-(Adamant-2-yl)benzenethiolato)(5-methoxycarbonyl-1,3-dimethylbenzimidazol-2-ylidene)] gold(I) (10a)

15.0 mg (23.3 μmol, 20%) from KO^{t}Bu (32.1 mg, 286 μmol, 2.00 eq.), **4** (28.0 mg, 114 μmol, 1.00 eq.) and **8a** (50.0 mg, 114 μmol, 1.00 eq.) in dry CH_2Cl_2 (10 mL). m.p. 150 °C (decomp.); ^{1}H NMR (500 MHz, $CDCl_3$) δ_H 8.18–8.14 (m, 2H, H^{ar}), 7.55–7.51 (m, 2H, H^{ar}), 7.49 (dd, J = 8.4 Hz, 0.7 Hz, 1H, H^{ar}), 7.07–7.02 (m, 2H, H^{ar}), 4.08 (d, J = 5.3 Hz, 6H, NMe), 3.98 (s, 3H, OMe), 2.90 (s, 1H, CH), 2.37 (d, J = 3.2 Hz, 2H, H^{ada}), 1.98 - 1.78 (m, 8H, H^{ada}), 1.73 (s, 4H, H^{ada}) ppm; ^{13}C NMR (125 MHz, $CDCl_3$) δ_C 192.3 (s, NCN), 166.4 (s, COOMe), 139.5 (s, C^{ar}), 137.7 (s, C^{ar}), 136.8 (s, C^{ar}), 133.8 (s, C^{ar}), 132.4 (s, C^{ar}), 126.8 (s, C^{ar}), 126.7 (s, C^{ar}), 126.1 (s, C^{ar}), 113.2 (s, C^{ar}), 111.1 (s, C^{ar}), 110.1 (s, C^{ar}), 52.8 (s, OMe), 46.4 (s, C^{ada}), 39.2 (s, C^{ada}), 38.1 (s, C^{ada}), 35.3 (s, NMe), 35.2 (s, NMe), 32.0 (s, C^{ada}), 31.1 (s, C^{ada}), 28.2 (s, C^{ada}), 27.9 (s, C^{ada}) ppm; HRMS (ESI): m/z calculated for $C_{13}H_{15}AuN_3O$ [(NHC)Au(MeCN)]$^+$: 442.08298. Found: 442.08198; m/z calculated for $C_{22}H_{24}AuN_4O_4$ [$(NHC)_2Au$]$^+$: 605.14631. Found: 605.14348; m/z calculated for $C_{38}H_{43}Au_2N_4O_4S$ [2 M-SPhAda]$^+$:1045.23361; Found: 1045.23011. Anal. Calcd. for $C_{27}H_{31}AuN_2O_2S$: C, 50.31; H, 4.85; N, 4.35, S, 4.97. Found: C, 49.76; H, 4.59; N, 4.19; S, 4.36.

[(4-(Adamant-2-yl)benzenethiolato)(5-methoxycarbonyl-1,3-diethylbenzimidazol-2-ylidene)] gold(I) (10b)

45.0 mg (67.0 μmol, 77%) from KO^{t}Bu (19.1 mg, 172 μmol, 2.00 eq.), **4** (21.1 mg, 86.2 μmol, 1.00 eq.) and **8b** (40.0 mg, 86.1 μmol, 1.00 eq.) in dry CH_2Cl_2 (7 mL). m.p. 150 °C (decomp.); ^{1}H NMR (500 MHz, $CDCl_3$) δ_H 8.24 (d, J = 1.3 Hz, 1H, H^{ar}), 8.19 (dd, J = 8.6 Hz, 1.3 Hz, 1H, H^{ar}), 7.62 (d, J = 8.6 Hz, 2H, H^{ar}), 7.56 (d, ^3J = 8.6 Hz, 1H, H^{ar}), 7.17–7.10 (m, 2H, H^{ar}), 4.64 (dq, J = 9.3 Hz, 7.3 Hz, 4H, NCH_2), 4.04 (s, 3H, OMe), 2.98 (s, 1H, CH), 2.44 (t, J = 3.2 Hz, 2H, H^{ada}), 2.06–1.86 (m, 4H, H^{ada}), 1.62 (q, 8H, CH_3, H^{ada}) ppm; ^{13}C NMR (125 MHz, $CDCl_3$) δ_C 191.3 (s, NCN), 166.4 (s, COOMe), 139.5 (s, C^{ar}), 138.0 (s, C^{ar}), 136.0 (s, C^{ar}), 133.0 (s, C^{ar}), 132.5 (s, C^{ar}), 126.7 (s, C^{ar}), 126.6 (s, C^{ar}),126.0 (s, C^{ar}), 113.4 (s, C^{ar}), 111.2 (s, C^{ar}), 52.8 (s, OMe), 46.4 (s, C^{ada}), 44.1 (d, J = 3.4 Hz, NCH_2), 39.3 (s, C^{ada}), 38.1 (s, NMe), 32.1 (s, NMe), 28.2 (s, C^{ada}), 28.0 (s, C^{ada}), 15.8 (s, CH_3), 27.9 (s, CH_3) ppm; HRMS (ESI): m/z calculated for $C_{15}H_{19}AuN_3O_2$ [(NHC)Au(MeCN)]$^+$: 470.11428. Found: 470.11294; m/z calculated for $C_{26}H_{32}AuN_4O_4$ [$(NHC)_2$Au]$^+$: 661.20891. Found: 661.20724; m/z calculated for $C_{42}H_{51}Au_2N_4O_4S$ [2 M-SPhAda]$^+$: 1101.29621; Found: 1101.29313.

[(4-(Adamant-2-yl)benzenethiolato)(5-methoxycarbonyl-1,3-dibenzylbenzimidazol-2-ylidene)] gold(I) (10c)

27.0 mg (33.4 μmol, 40%) from KO^{t}Bu (23.8 mg, 212 μmol, 2.00 eq.), **4** (20.8 mg, 84.9 μmol, 1.00 eq.) and **8c** (50.0 mg, 84.9 μmol, 1.00 eq.) in dry CH_2Cl_2 (7 mL). m.p. 175 °C (decomp.); ^{1}H NMR (500 MHz, $CDCl_3$) δ_H 8.09 (d, J = 1.4 Hz, 1H, H^{ar}), 8.01 (dd, J = 8.6 Hz, 1.4 Hz, 1H, H^{ar}), 7.48 (d, J = 8.1 Hz, 2H, H^{ar}), 7.44 (dd, J = 7.6 Hz, 1.7 Hz, 2H, H^{ar}), 7.40 (d, J = 6.6 Hz, 3H, H^{ar}), 7.36–7.30 (m, 6H, H^{ar}), 6.99 (d, J = 8.0 Hz, 2H, H^{ar}), 5.79 (d, J = 3.2 Hz, 4H, NCH_2), 3.91 (s, 3H, OMe) 2.90 (s, 1H, CH), 2.36 (d, J = 3.9 Hz, 2H, H^{ada}), 1.99–1.86 (m, 6H, H^{ada}), 1.82–1.77 (m, 3H, H^{ada}) 1.74 (s, 3H, H^{ada}) ppm; ^{13}C NMR (125 MHz, $CDCl_3$) δ_C 192.7 (s, NCN), 166.1 (s, COOMe), 139.3 (s, C^{ar}), 137.5 (s, C^{ar}), 136.3 (s, C^{ar}), 134.4 (s, C^{ar}), 134.3 (s, C^{ar}), 133.4 (s, C^{ar}), 132.5 (s, C^{ar}), 129.2 (s, C^{ar}), 128.7 (s, C^{ar}), 127.5 (s, C^{ar}), 126.8 (s, C^{ar}), 126.6 (s, C^{ar}), 126.1 (s, C^{ar}), 113.82 (s, C^{ar}), 111.9 (s, C^{ar}), 52.9 (s, NCH_2), 52.7 (s, NCH_2), 52.6 (s, OMe), 46.3 (s, C^{ada}), 39.2 (s, NCH_2), 38.0 (s, C^{ada}), 31.9 (s, NMe), 31.0 (s, NMe), 28.1 (s, C^{ada}), 27.8 (s, C^{ada}) ppm; HRMS (ESI): m/z calculated for $C_{20}H_{21}AuN_3O_2$ [NHC)Au(MeCN]$^+$: 594.14558. Found: 594.14365; m/z calculated for $C_{46}H_{40}AuN_4O_4$ [$(NHC)_2$Au]$^+$: 909.27151. Found: 909.26784; m/z calculated for $C_{62}H_{59}Au_2N_4O_4S$ [2 M-SPhAda]$^+$ 1349.35881; Found: 1349.35422.

[Chlorido(5-(4-(adamant-1-yl)phenoxycarbonyl)-1,3-diethylbenzimidazol-2-ylidene)]gold(I) (17)

A solution of **16** (100 mg, 180 μmol, 1.00 eq.) in dry CH_2Cl_2 (10 mL) was treated with Ag_2O (25.0 mg, 108 μmol, 0.60 eq.), stirred at rt for 6 h while being shielded from light, and finally treated with AuCl(SMe_2) (58.2 mg, 198 μmol, 1.10 eq.) and LiCl (76.2 mg, 1.80 mmol, 10.0 eq.). The mixture was left stirring for another 24 h, filtered over Celite, and concentrated in vacuo. The residue was purified by column chromatography (cyclohexane/EtOAc; 1:1) to afford **17** as a colourless powder (78.0 mg, 118 μmol, 66%) with R_f 0.67 and m.p. 310 °C (decomp.); ^{1}H NMR (500 MHz, $CDCl_3$) δ_H 8.35 (s, 1H, H^{ar}), 8.31 (d, J = 8.6, 1H, H^{ar}), 7.59 (d, J = 8.5 Hz, 1H, H^{ar}), 7.44 (d, J = 8.4 Hz, 2H, H^{ar}), 7.18 (d, J = 8.8 Hz, 2H, H^{ar}), 4.60 (dq, J = 7.3 Hz, 7.2 Hz, 4H, NCH_2), 2.12 (s, 3H, H^{ada}), 1.93 (s, 6H, H^{ada}), 1.78 (q, J = 12.5 Hz, 6H, H^{ada}), 1.58 (dt, J = 11.6 Hz, 5.7 Hz, 6H) ppm; ^{13}C NMR (125 MHz, $CDCl_3$) δ_C 180.7 (NCN), 164.5 (s, COOR), 149.5 (s, C^{ar}), 148.3 (s, C^{ar}), 136.0 (s, C^{ar}), 132.8 (s, C^{ar}), 126.5 (s, C^{ar}), 126.3 (s, C^{ar}), 126.2 (s, C^{ar}), 120.9 (s, C^{ar}), 113.9 (s, C^{ar}), 111.3 (s, C^{ar}), 44.3 (d, J = 2.7 Hz, NCH_2), 43.3 (s, C^{ada}), 36.7 (s, C^{ada}), 36.1 (s, C^{ada}), 28.9 (s, C^{ada}), 15.6 (d, J = 22.6 Hz, CH_3) ppm; HRMS (ESI): m/z calculated for $C_{30}H_{35}AuN_3O_2$ [(NHC)Au(MeCN)]$^+$: 666.23948. Found: 666.23766; Anal. Calcd. for $C_{28}H_{32}AuClN_2O_2$: C, 50.88; H, 4.88; N, 4.24. Found: C, 49.55; H, 4.90; N, 3.73.

(5-(((2,3-dimethylcycloprop-2-en-1-yl)methoxy)carbonyl)-1,3-diethylbenzimidazol-2-ylidene gold(I) thiophenolato (20)

A solution of complex **19** (60.0 mg, 113 μmol, 1.00 eq.) in dry CH_2Cl_2 (10 mL) was treated with KO^{t}Bu (15.2 mg, 136 μmol, 1.20 eq.), left stirring for 1 h at rt, and then treated with thiophenol (12.2 μL, 120 μmol, 1.06 eq.). After stirring at rt for 24 h, the suspension was filtered, and the solvent was evaporated. The residue was precipitated from *n*-pentane to leave the product complex as a yellowish powder (56.0 mg, 92.6 μmol, 82%) after filtration and drying in vacuo; m.p. 110 °C; ^{1}H NMR (500 MHz, $CDCl_3$) δ_H 8.21 (d, J = 1.4 Hz, 1H, H^{ar}), 8.16 (dd, J = 8.5 Hz, 1.4 Hz, 1H, H^{ar}), 7.64 (dd, J = 8.3 Hz, 1.2 Hz, 2H, H^{ar}), 7.51 (d, J = 8.5 Hz, 1H, H^{ar}), 7.10 (t, J = 7.7 Hz, 2H, H^{ar}), 6.97 (d, J = 7.3 Hz, 1H, H^{ar}), 4.59 (dq, J = 11.2 Hz, 7.3 Hz, 4H, NCH_2), 4.28 (d, J = 5.2 Hz, 2H, CH_2), 2.04 (s, 6H, CH_3), 1.69 (t, J = 5.2 Hz, 1H, CH), 1.58 (dt, J = 9.3 Hz, 7.3 Hz 6H, CH_3) ppm; ^{13}C NMR (125 MHz, $CDCl_3$) δ_C 190.8 (s, NCN), 166.0 (s, $COOCH_2$), 142.3 (s, C^{ar}), 135.7 (s, C^{ar}), 132.9 (s, C^{ar}), 132.6 (s, C^{ar}), 128.0 (s, C^{ar}), 127.5 (s, C^{ar}), 125.8 (s, C^{ar}), 123.2 (s, C^{ar}), 113.2 (s, C^{ar}), 110.9 (s, C^{ar}), 109.7 (s, C=C), 73.2 (s, OCH_2), 44.0 (d, J = 2.7 Hz, CH_3), 19.3 (s, CH), 15.7 (d, J = 15.4 Hz, CH_3), 10.5 (s, CH_3) ppm; HRMS (ESI): m/z calculated for $C_{20}H_{25}AuN_3O_2$ [NHC)Au(MeCN]$^+$: 536.16123. Found: 536.15792; m/z calculated for $C_{36}H_{44}AuN_4O_4$ [$(NHC)_2$Au]$^+$: 793.30281. Found: 793.29786; m/z calculated for $C_{42}H_{49}Au_2N_4O_4S$ [2 M-SPhAda]$^+$ 1099.28056; Found: 1099.27465; Anal. Calcd. for $C_{24}H_{27}AuN_2O_2S$: C, 47.68; H, 4.50; N, 4.63, S, 5.30. Found: C, 47.30; H, 4.32; N, 4.41; S, 5.36.

[(4-(Adamant-2-yl)benzenethiolato(5-((2,3-dimethylcycloprop-2-en-1-yl)methoxycarbonyl)-1,3-diethylbenzimidazol-2-ylidene)] gold(I) (21)

A solution of complex **19** (40.0 mg, 75.4 μmol, 1.00 eq.) in dry CH_2Cl_2 (7 mL) was treated with KO^{t}Bu (16.9 mg, 151 μmol, 2.00 eq.), left stirring for 1 h at rt, and then treated with thiol **4** (18.4 mg, 75.4 μmol, 1.00 eq.). After stirring at rt for 48 h, the suspension was filtered over Celite, and the solvent was evaporated. The residue was precipitated from *n*-pentane to afford the product complex as a brown powder (40.0 mg, 54.1 μmol, 72%) after filtration and drying in vacuo; m.p. 160 °C; ^{1}H NMR (500 MHz, $CDCl_3$) δ_H 8.20 (d, J = 1.4 Hz, 1H, H^{ar}), 8.16 (dd, J = 8.5 Hz, 1.4 Hz, 1H, H^{ar}), 7.56 (d, J = 8.2 Hz, 2H, H^{ar}), 7.51 (d, J = 8.6 Hz, 1H, H^{ar}), 7.07 (d, J = 8.0 Hz, 2H, H^{ar}), 4.58 (dq, J = 9.1 Hz, 7.3 Hz, 4H, NCH_2), 4.20 (d, J = 5.2 Hz, 2H, CH_2), 2.91 (s, 1H, H^{ada}), 2.38 (s, 2H, H^{ada}), 2.03 (s, 6H, CH_3), 1.97–1.64 (m, 4H, H^{ada}), 1.92–1.87 (m, 2H, H^{ada}), 1.85–1.78 (m, 2H, CH^{ada}), 1.73 (s, 3H, H^{ada}),1.68 (t, J = 5.2 Hz, 1H, CH), 1.57 (dt, J = 9.3 Hz, 7.3 Hz 6H, CH_3), 1.51 (s, 1H, H^{ada}) ppm; ^{13}C NMR (125 MHz, $CDCl_3$) δ_C 192.1 (s, NCN), 166.0 (s, $COOCH_2$), 139.5 (s, C^{ar}), 135.8 (s, C^{ar}), 135.6 (s, C^{ar}), 132.8 (s, C^{ar}), 132.3 (s, C^{ar}), 127.5 (s, C^{ar}), 126.6 (s, C^{ar}), 125.8 (s, C^{ar}), 113.2 (s, C^{ar}), 111.0 (s, C^{ar}), 109.7 (s, C=C), 73.3 (s, OCH_2), 46.3 (s, CH), 44.0 (d, J = 3.6 Hz, CH_3), 39.1 (s, C^{ada}), 38.0 (s, C^{ada}), 31.9 (s, C^{ada}), 31.0 (s, C^{ada}), 28.1 (s, C^{ada}), 27.8 (s, C^{ada}), 19.3 (s, CH), 15.7 (d, J = 14.5 Hz, CH_3), 10.5 (s, CH_3) ppm. HRMS (ESI): m/z calculated for $C_{20}H_{25}AuN_3O_2$ [NHC)Au(MeCN]$^+$: 536.16123. Found: 536.15792; m/z calculated for $C_{36}H_{44}AuN_4O_4$ [$(NHC)_2$Au]$^+$: 793.30281. Found: 793.29786; m/z calculated for $C_{52}H_{63}Au_2N_4O_4S$ [2 M-SPhAda]$^+$ 1233.39011; Found: 1233.38487. Anal. Calcd. for $C_{34}H_{41}AuN_2O_2S$: C, 55.28; H, 5.59; N, 3.79, S, 4.34. Found: C, 56.62; H, 4.93; N, 3.69; S, 3.70.

Supporting Information

The synthetic protocols, datasets and spectra of the products, as well as biological assays and their results were uploaded as part of the supplementary material.

Additional references cited within the Supporting Information.[41–47]

Acknowledgements

R. S. thanks the Deutsche Forschungsgemeinschaft (DFG) for a grant (Scho 402/12-2). We thank Dr. Ulrike Lacher for measuring and analysing mass spectra, Anthony Putratama for synthesising precursors and Dr. Obst for the ICP-MS measurements. Open Access funding enabled and organized by Projekt DEAL.

Conflict of Interests

There are no conflicts to declare.

Data Availability Statement

The data that support the findings of this study are available from the corresponding author upon reasonable request.

Keywords: antitumor agents · bioorthogonal click chemistry · gold · NHC complexes · medicinal chemistry

[1] D. Hanahan, *Cancer Dis.* **2022**, *12*, 31–46.
[2] a) D. W. Shen, L. M. Pouliot, M. D. Hall, M. M. Gottesman, *Pharmacol. Rev.* **2012**, *64*, 706–721; b) J. Zhou, Y. Kang, L. Chen, H. Wang, J. Liu, S. Zeng, L. Yu, *Front. Pharmacol.* **2020**, *11*.
[3] M. Höckel, P. Vaupel, *J. Natl. Cancer Inst.* **2001**, *93*, 266–276.
[4] S. J. Yeung, J. Pan, M. H. Lee, *Cell. Mol. Life Sci.* **2008**, *65*, 3981–3999.
[5] S. H. Li, D. H. Shin, Y.-S. Chun, M. K. Lee, M.-S. Kim, J.-W. Park, *Mol. Cancer Ther.* **2008**, *7*, 3729–3738.
[6] D. Bhattarai, X. Xu, K. Lee, *Med. Res. Rev.* **2018**, *38*, 1404–1442.
[7] M.-S. Won, N. Im, S. Park, S. K. Boovanahalli, Y. Jin, X. Jin, K.-S. Chung, M. Kang, K. Lee, S.-K. Park, H. M. Kim, B. M. Kwon, J. J. Lee, K. Lee, *Biochem. Biophys. Res. Commun.* **2009**, *385*, 16–21.
[8] a) S. I. Bär, M. Gold, S. W. Schleser, T. Rehm, A. Bär, L. Köhler, L. R. Carnell, B. Biersack, R. Schobert, *Chem. Eur. J.* **2021**, *27*, 5003–5010; b) A. Nguyen, A. Vessières, E. Hillard, S. Top, P. Pigeon, G. Jaouen, *Chimia* **2007**, *61*, 716–724; c) S. Knauer, B. Biersack, M. Zoldakova, K. Effenberger, W. Milius, R. Schobert, *Anti-Cancer Drugs* **2009**, *20*, 676–681; d) R. A. Sánchez-Delgado, A. Anzellotti, L. Suárez, *Met. Ions Biol. Syst.* **2004**, *41*, 379–419; e) L. Kober, S. W. Schleser, S. I. Bär, R. Schobert, *J. Biol. Inorg. Chem.* **2022**, *27*, 731–745; f) S. W. Schleser, H. Ghosh, G. Hörner, J. Seib, S. Bhattacharyya, B. Weber, R. Schobert, P. Dandawate, B. Biersack, *Int. J. Mol. Sci.* **2023**, *24*, 5738.
[9] a) W. Fiskus, N. Saba, M. Shen, M. Ghias, J. Liu, S. D. Gupta, L. Chauhan, R. Rao, S. Gunewardena, K. Schorno, C. P. Austin, K. Maddocks, J. Byrd, A. Melnick, P. Huang, A. Wiestner, K. N. Bhalla, *Cancer Res.* **2014**, *74*, 2520–2532; b) P. V. Raninga, A. C. Lee, D. Sinha, Y.-Y. Shih, D. Mittal, A. Makhale, A. L. Bain, D. Nanayakarra, K. F. Tonissen, M. Kalimutho, K. K. Khanna, *Int. J. Cancer* **2020**, *146*, 123–136; c) C. Marzano, V. Gandin, A. Folda, G. Scutari, A. Bindoli, M. P. Rigobello, *Free Radical Biol. Med.* **2007**, *42*, 872–881.
[10] a) X. Zhang, K. Selvaraju, A. A. Saei, P. D'Arcy, R. A. Zubarev, E. S. J. Arnér, S. Linder, *Biochimie* **2019**, *162*, 46–54; b) P. Zou, M. Chen, J. Ji, W. Chen, X. Chen, S. Ying, J. Zhang, Z. Zhang, Z. Liu, S. Yang, G. Liang, *Oncotarget* **2015**, *6*.
[11] a) S. M. Meier-Menches, B. Neuditschko, K. Zappe, M. Schaier, M. C. Gerner, K. G. Schmetterer, G. Del Favero, R. Bonsignore, M. Cichna-Markl, G. Koellensperger, A. Casini, C. Gerner, *Chem. Eur. J.* **2020**, *26*, 15528–15537; b) G. Gorini, F. Magherini, T. Fiaschi, L. Massai, M. Becatti, A. Modesti, L. Messori, T. Gamberi, *Biomedicine* **2021**, *9*, 871; c) L. K. Webster, S. Rainone, E. Horn, E. R. Tiekink, *Met.-Based Drugs* **1996**, *3*, 63–66; d) C. Schmidt, B. Karge, R. Misgeld, A. Prokop, R. Franke, M. Brönstrup, I. Ott, *Chem. Eur. J.* **2017**, *23*, 1869–1880.
[12] H. Uchiro, S. Kobayashi, *Tetrahedron Lett.* **1999**, *40*, 3179–3182.
[13] D. L. Kokkin, R. Zhang, T. C. Steimle, I. A. Wyse, B. W. Pearlman, T. D. Varberg, *J. Phys. Chem. A* **2015**, *119*, 11659–11667.
[14] S. I. Bär, S. W. Schleser, N. Oberhuber, A. Herrmann, L. Schlotte, S. E. Weber, R. Schobert, *J. Inorg. Biochem.* **2022**, *238*, 112028.
[15] T. Onodera, I. Momose, M. Kawada, *Chem. Pharm. Bull.* **2019**, *67*, 186–191.
[16] D. W. Shen, C. Cardarelli, J. Hwang, M. Cornwell, N. Richert, S. Ishii, I. Pastan, M. M. Gottesman, *J. Biol. Chem.* **1986**, *261*, 7762–7770.
[17] H. Yang, R. M. Villani, H. Wang, M. J. Simpson, M. S. Roberts, M. Tang, X. Liang, *J. Exp. Clin. Cancer Res.* **2018**, *37*, 266.
[18] G.-Y. Liou, P. Storz, *Free Radical Res.* **2010**, *44*, 479–496.
[19] R. P. Rastogi, S. P. Singh, D. P. Häder, R. P. Sinha, *Biochem. Biophys. Res. Commun.* **2010**, *397*, 603–607.
[20] M. C. C. Sachweh, W. C. Stafford, C. J. Drummond, A. R. McCarthy, M. Higgins, J. Campbell, B. Brodin, E. S. J. Arnér, S. Laín, *Oncotarget* **2015**, *6*.
[21] H. Hwang-Bo, J. W. Jeong, M. H. Han, C. Park, S. H. Hong, G. Y. Kim, S. K. Moon, J. Cheong, W. J. Kim, Y. H. Yoo, Y. H. Choi, *Gen. Physiol. Biophys.* **2017**, *36*, 117–128.
[22] J. Bartek, C. Lukas, J. Lukas, *Nat. Rev. Mol. Cell Biol.* **2004**, *5*, 792–804.
[23] J. E. Leadsham, V. N. Kotiadis, D. J. Tarrant, C. W. Gourlay, *Cell Death Differ.* **2010**, *17*, 754–762.
[24] V. E. Franklin-Tong, C. W. Gourlay, *Biochem. J.* **2008**, *413*, 389–404.
[25] J. C. Mills, N. L. Stone, R. N. Pittman, *J. Cell Biol.* **1999**, *146*, 703–708.
[26] B. Huppertz, H.-G. Frank, P. Kaufmann, *Anat. Embryol.* **1999**, *200*, 1–18.
[27] K. Bertheussen, M. van de Plassche, T. Bakkum, B. Gagestein, I. Ttofi, A. J. C. Sarris, H. S. Overkleeft, M. van der Stelt, S. I. van Kasteren, *Angew. Chem. Int. Ed.* **2022**, *61*, e202207640.
[28] a) S. Fulda, L. Galluzzi, G. Kroemer, *Nat. Rev. Drug Discovery* **2010**, *9*, 447–464; b) P. E. Porporato, N. Filigheddu, J. M. B.-S. Pedro, G. Kroemer, L. Galluzzi, *Cell Res.* **2018**, *28*, 265–280.
[29] Y. Yang, S. Karakhanova, W. Hartwig, J. G. D'Haese, P. P. Philippov, J. Werner, A. V. Bazhin, *J. Cell. Physiol.* **2016**, *231*, 2570–2581.
[30] a) F. Hecht, C. F. Pessoa, L. B. Gentile, D. Rosenthal, D. P. Carvalho, R. S. Fortunato, *Tumor Biol.* **2016**, *37*, 4281–4291; b) M. Ushio-Fukai, Y. Nakamura, *Cancer Lett.* **2008**, *266*, 37–52; c) P. Wigner, R. Grębowski, M. Bijak, J. Saluk-Bijak, J. Szemraj, *Int. J. Mol. Sci.* **2021**, *22*.
[31] J. Folkman, *Semin. Oncol.* **2002**, *29*, 15–18.
[32] G. U. Dachs, G. M. Tozer, *Eur. J. Cancer* **2000**, *36*, 1649–1660.
[33] E. Aranda, G. Owen, *Biol. Res.* **2009**, *42*, 377–389.
[34] E. J. Yeo, Y. S. Chun, J. W. Park, *Biochem. Pharmacol.* **2004**, *68*, 1061–1069.
[35] M. Mora, M. C. Gimeno, R. Visbal, *Chem. Soc. Rev.* **2019**, *48*, 447–462.
[36] a) M. Safir Filho, T. Scattolin, P. Dao, N. V. Tzouras, R. Benhida, M. Saab, K. Van Hecke, P. Lippmann, A. R. Martin, I. Ott, S. P. Nolan, *New J. Chem.* **2021**, *45*, 9995–10001; b) A. A. A. Sulaiman, N. Kalia, G. Bhatia, M. Kaur, M. Fettouhi, M. Altaf, N. Baig, A.-N. Kawde, A. A. Isab, *New J. Chem.* **2019**, *43*, 14565–14574; c) T. Scattolin, P. Lippmann, M. Beliš, K. van Hecke, I. Ott, S. P. Nolan, *Appl. Organomet. Chem.* **2022**, *n/a*, e6624; d) R. Visbal, V. Fernández-Moreira, I. Marzo, A. Laguna, M. C. Gimeno, *Dalton Trans.* **2016**, *45*, 15026–15033.
[37] M. Idelchik, U. Begley, T. J. Begley, J. A. Melendez, *Semin. Cancer Biol.* **2017**, *47*, 57–66.
[38] D. K. Orren, L. N. Petersen, V. A. Bohr, *Mol. Biol. Cell* **1997**, *8*, 1129–1142.
[39] J. Rao, N. Li, *Curr. Cancer Drug Targets* **2004**, *4*, 345–354.
[40] H. Draut, T. Rehm, G. Begemann, R. Schobert, *Chem. Biodiversity* **2017**, *14*, e1600302.
[41] J. J. Dunsford, E. R. Clark, M. J. Ingleson, *Angew. Chem. Int. Ed.* **2015**, *54*, 5688–5692.
[42] Z. Zhang, P. Chaltin, A. Van Aerschot, J. Lacey, J. Rozenski, R. Busson, P. Herdewijn, *Bioorg. Med. Chem.* **2002**, *10*, 3401–3413.

[43] L. H. F. Köhler, S. Reich, G. Begemann, R. Schobert, B. Biersack, *ChemMedChem* **2022**, *17*, e202200064.
[44] B. Linder, L. H. F. Köhler, L. Reisbeck, D. Menger, D. Subramaniam, C. Herold-Mende, S. Anant, R. Schobert, B. Biersack, D. Kögel, *Biomol. Eng.* **2021**, *11*.
[45] O. Dolomanov, L. Bourhis, R. Gildea, J. Howard, H. Puschmann, *J. Appl. Cryst. J. Appl. Cryst* **2009**, *42*, 339–341.
[46] G. M. Sheldrick, *Acta Crystallogr A Found Adv* **2015**, *71*, 3–8.
[47] C. F. Macrae, I. Sovago, S. J. Cottrell, P. T. A. Galek, P. McCabe, E. Pidcock, M. Platings, G. P. Shields, J. S. Stevens, M. Towler, P. A. Wood, *J. Appl. Crystallogr.* **2020**, *53*, 226–235.

Manuscript received: April 3, 2023
Revised manuscript received: May 9, 2023
Accepted manuscript online: May 10, 2023